Procedia Computer Science
Volume 51, 2015, Pages 1534–1544
ICCS 2015 International Conference On Computational Science

Numerical verification criteria for coseismic and postseismic crustal deformation analysis with large-scale high-fidelity model

Ryoichiro Agata[1][2], Tsuyoshi Ichimura[3], Kazuro Hirahara[4],
Mamoru Hyodo[5], Takane Hori[5], Chihiro Hashimoto[6], and Muneo Hori[3]

[1] Department of Civil Engineering, The University of Tokyo, Tokyo, Japan
agata@eri.u-tokyo.ac.jp
[2] Research Fellow of the Japan Society for the Promotion of Science
[3] Earthquake Research Institute, The University of Tokyo, Tokyo, Japan
ichimura@eri.u-tokyo.ac.jp, hori@eri.u-tokyo.ac.jp
[4] Kyoto University, Kyoto, Japan
hirahara@kugi.kyoto-u.ac.jp
[5] Japan Agency for Marine-Earth Science and Technology, Yokohama, Japan
hyodo@jamstec.go.jp, horit@jamstec.go.jp
[6] Nagoya University, Aichi, Japan
hashi@seis.nagoya-u.ac.jp

Abstract
Numerical verification of postseismic crustal deformation analysis, computed using a large-scale finite element simulation, was carried out, by proposing new criteria that consider the characteristics of the target phenomenon. Specifically, pointwise displacement was used in the verification. In addition, the accuracy of the numerical solution was explicitly shown by considering the observation error of the data used for validation. The computational resource required for each analysis implies that high-performance computing techniques are necessary to obtain a verified numerical solution of crustal deformation analysis for the Japanese Islands. Such verification in crustal deformation simulations should take on greater importance in the future, since continuous improvement in the quality and quantity of crustal deformation data is expected.

Keywords:

1 Introduction

Numerical simulation is widely used in science and engineering. To assure the quality of results obtained by numerical simulation, a process known as ”verification and validation (V&V)” has been proposed[18]. Verification is a process that checks whether a numerical model assumed for a certain

Selection and peer-review under responsibility of the Scientific Programme Committee of ICCS 2015
© The Authors. Published by Elsevier B.V.

doi:10.1016/j.procs.2015.05.344

physical phenomenon (e.g., a partial differential equation) is solved correctly by the simulation code. This process is typically used for setting an appropriate discretization size, within which the numerical solution converges. Validation is a process that checks whether the numerical model reasonably explains the target physical phenomenon. This classification avoids confusion when discussing differences between results of numerical solutions and actual observation data.

In the field of solid earth science, coseismic (during an earthquake) and postseismic (after an earthquake) crustal deformation due to fault dislocation in a subduction zone has been studied. The time and spatial scale of the deformation is of the order of $10^0 \sim 10^1$ years and 10^3km $\times$ 10^3km horizontally, respectively. Many studies have used analytical solutions with simplified structures [14][4] to calculate crustal deformation, since analytical solutions do not require the same computational power as numerical solutions. However, since interplate faulting in a subduction zone has a complex and heterogeneous three-dimensional (3D) structure, numerical simulation methods; e.g., finite element (FE) methods, are suitable for analyzing deformation around this system. Some recent studies attempted to use an FE model at a relatively low resolution to include the 3D structure of the subduction zone in the simulation [12] [17]. Ongoing development of observational techniques has yielded more detailed data on crustal deformation and crustal structure. In Japan, for example, crustal deformation data have been collected by GEONET [5], the observation error of which is of the order of mm. In focal regions of subduction earthquakes, some observation systems are already in service with observation errors of the order of cm (e.g., DONET [10]). Detailed geometric data of 3D heterogeneous crustal structure are also available in those focal regions (e.g., Koketsu et al. [11]). Crustal deformation data are used for validation of numerical simulation results or inversion analysis of earthquake fault slips, while crustal structure data are applied to construction of numerical simulation models. It is desirable to carry out simulations of crustal deformation at a resolution and accuracy similar to those data, at the appropriate time and spatial scales for the target problem. This is not, however, an easy task: even with the newest computational environments, construction of simulation models and performing the simulation itself becomes computationally costly.

To overcome the problem of computational cost, high-performance computing (HPC) is necessary. Ichimura et al. [9] developed a tool to compute coseismic and postseismic crustal deformation on a large-scale computer such as the K computer, currently the fastest supercomputer in Japan, using an FE model of similar high-fidelity to the crustal structure data (HFM: high-fidelity model). That paper mainly discussed a fast and scalable computational method. We expect that such a high-fidelity crustal deformation simulation method will become a standard tool for analyzing crustal deformation, as more global crustal structure data of subduction zones are expected to be available in the future. To discuss the necessity for high-fidelity analysis, it is also important to examine the quality of simulation results. However, none of the verification methods used in other fields are applicable to the target simulation. For instance, the typical verification methods used in computer-aided engineering (CAE) are based on stress distribution [8]. In computational seismology, some studies (e.g., Martin [3]) used criteria to quantify the level of agreement between two wave forms such as the goodness-of-fit scores [2]. These verification criteria are not applicable to the characteristics of crustal deformation simulations; the simulation results need to be compared with pointwise displacement data spread across a wide area.

In this paper, we seek to carry out verification of the numerical solutions computed in [9] by checking the convergence of the numerical solution. To clarify the accuracy of the results which the problem setting provides, we propose new verification criteria that are more suitable for the characteristics of the crustal deformation simulation mentioned above. For the evaluation of accuracy, we also consider the observation error of crustal deformation data to be used for validation, inversion analysis of earthquake fault slip, etc. We also discuss the computation time for the target simulation to show that HPC facilities are essential to assure the quality of the simulation results.

2 Target problem

Details of the target problem for verification are provided in Ichimura et al. [9], and described briefly here. We describe coseismic and postseismic crustal deformation as linear elasticity and the Maxwell model of viscoelasticity, as:

$$\begin{aligned}
&\sigma_{ij,j} + f_i = 0,\\
&\dot{\sigma}_{ij} = \lambda\dot{\epsilon}_{kk}\delta_{ij} + 2\mu\dot{\epsilon}_{ij} - \frac{\mu}{\eta}(\sigma_{ij} - \frac{1}{3}\sigma_{kk}\delta_{ij}),\\
&\epsilon_{ij} = \frac{1}{2}(u_{i,j} + u_{j,i}).
\end{aligned}$$

Here, σ_{ij}, f_i are the stress tensor and outer force. $(\dot{\ }), (\ )_{,i}, \delta_{ij}, \eta, \epsilon_{ij}, u_i$ are first-order derivative in time, first-order derivative in the ith coordinate, Kronecker delta, viscosity coefficient, strain tensor and displacement, respectively. λ, μ are Lame's constants. These governing equations are for the Maxwell model, and equivalent to those of linear elasticity when $\eta = \infty$. Since the equations do not include the acceleration term, the problem can be solved as a quasi-static problem, and so a larger time-step length can typically be taken. We used an FE method to solve the equation using the formulation of Parker et al. [15], after which the problem becomes equivalent to the solution of a linear equation in $\mathbf{Ku} = \mathbf{f}$ for each time step. Earthquake fault slip was introduced by using the split-node technique [13], and Dirichlet boundary conditions were imposed at the sides and bottom of the target domain. Specifically, displacements in the normal direction at points on the side and bottom planes are fixed to zero, while there are no imposed values in other directions [1]. To solve $\mathbf{Ku} = \mathbf{f}$ on a large-scale supercomputer such as the K computer, Ichimura et al. [9] developed a scalable and fast linear solver. The basic algorithm consists of a Conjugate Gradient method and Element-by-Element method [13] to achieve memory efficiency. To improve the convergence of the CG solver, an adaptive preconditioner was used in combination with a multigrid approach based on elements of different polynomial orders. The code was parallelized using both Message Passing Interface (MPI) and OpenMP (hybrid parallelization). We computed response displacement due to a point source in a multilayered elastic/visco elastic half–space using the method above, and compared the numerical solution with an analytical solution computed using the method of Fukahata and Matsu'ura [4]. We found our numerical solution agreed well with the analytical solution [9].

The target problem is a simulation of coseicmic and postseismic crustal deformation of the Japanese Islands due to the 2011 Tohoku-oki Earthquake. The target domain for the analysis is shown in Figure 1. To carry out FE analyses, we need geometry data for the crustal structure of the Japanese Islands, to construct an FE mesh. For the ground surface, JTOPO30, an elevation data set in 900-m resolution, was used. For the Philippine Sea Plate and Pacific Plate, two types of data were applied: For the focal region, the detailed data of Koketsu et al. [11] were used, whereas the CAMP model [6] was used elsewhere. The thickness of the elastic layer of the continental plate and the elastic slab of the Philippine Sea Plate were set to be 30 km, and the elastic slab of the Pacific Plate to be 80 km. Viscoelastic layers were located below each elastic layer. The viscosity of the viscoelastic layers was set to be $\eta = 5 \times 10^{18}$Pa s following Hashimoto et al. [6]. For FE mesh construction for HFM, we used a meshing technique using a background grid[9]. This method allows to set an arbitrary mesh resolution ds in the interface between each layer, with slight approximation of geometry to maintain the mesh quality. At the same time, unnecessary elements are merged to generate larger elements elsewhere. A quadratic tetrahedral element type was used (Figure 2). Hereafter, "mesh size" also refers to "ds", the resolution of the layer interface. Figure 3 shows the FE model constructed for the target area. The mesh is constructed in a Cartesian coordinate system. The target area is $0 \leq x \leq 2944$ km west-to-east, $0 \leq y \leq 2752$ km south–to–north, and $-850 \leq z \leq 0$ km vertically. In construction of the basic settings used hereonin,

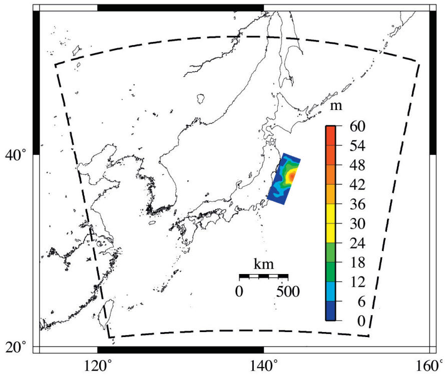
m
60
54
48
42
36
30
24
18
12
6
0
km
0
500
40°
20°
120°
140°
160°

Figure 1: The target domain for our simulation (black dashed line) and the input fault slip of the 2011 Tohoku-oki Earthquake[20] (color contour).

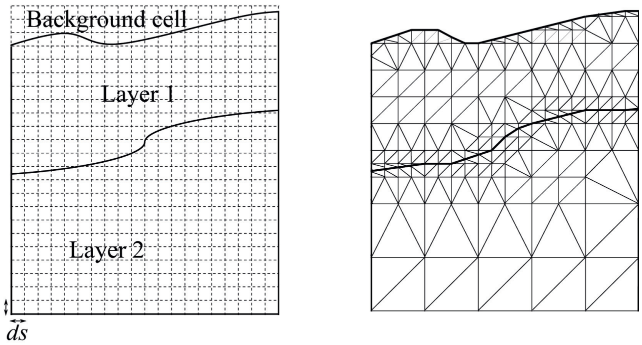
Background cell
Layer 1
Layer 2
ds

(a)Input data and background grid (b)Constructed FE mesh

Figure 2: Two–dimensional schematics of FE mesh construction for HFM. We set arbitrary resolution of mesh ds in the interface between each layer by using background grid. At the same time, unnecessary elements are merged to generate larger elements elsewhere. The element type is quadratic tetrahedral element.

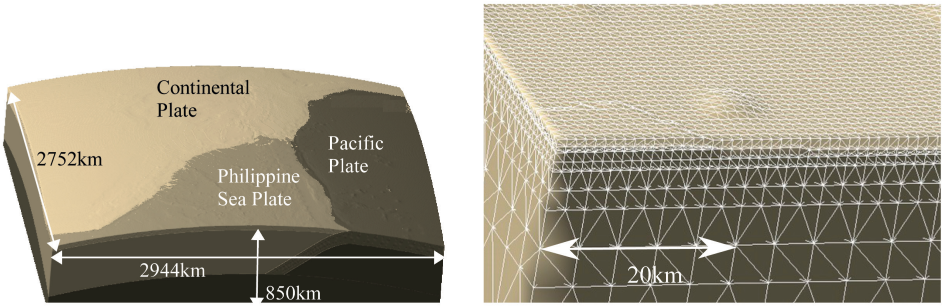
Continental
Plate
Pacific
Plate
Philippine
Sea Plate
2752km
2944km
850km
20km

Overview Close-up view

Figure 3: HFM constructed in the target domain. The ground surface is divided by the plate for the continent, Philippine Sea Plate, and Pacific Plate. The close-up view shows that the FE mesh represents the geometry of each layer in details.

the degrees-of-freedom of the FE model was 9,997,100,409, and the number of quadratic tetrahedral elements was 2,479,581,830. For earthquake fault slip in the 2011 Tohoku-oki Earthquake, we input the fault-slip distribution estimated by Yagi et al. [20] onto the fault plane of this model. The location of the fault plane is also shown in Figure 1.

3 Evaluation method of accuracy

The goal of verification is to estimate the numerical error caused by the discretization [18]. Studies of FE analyses often use Richardson extrapolation for this purpose, by using numerical solutions with different descretization sizes to analyze convergence rate [16]. On the other hand, approximation of geometry is necessary to maintain the mesh quality in the process of constructing FE mesh in such a large domain as our target, as mentioned in Section 2. We have confirmed that numerical solutions computed by our method approaches certain values as the discretization size gets smaller, by drawing convergence curve associated with our numerical solution. However, we also found that slight change in geometry is sensitive to the convergence curve with respect to the discretization sizes, which made it difficult to apply error analysis using Richardson extrapolation to our computation method. Thus we need an alternative verification strategy, and so made it as following. Based on the fact that the numerical solution approaches to certain value as the discretization size gets smaller, we seek to find certain spatial discretization size with which the error is expected to be sufficiently small. We used the same approach for the time step length and the domain size. Here, for simplicity, we firstly present basic settings based on some prescribed analyses. By comparing the solution using basic settings with those of a different mesh size, time-step length and target domain, we show convergence of the solution using basic settings. For the basic settings, ds=1000m, dt=30days, and the target domain is that shown in Figure 1. Here we define Model A as an FE model with the same parameters as the basic model but with ds=750m, Model B as an FE model with the same parameters as the basic model but with dt=15days and Model C as an FE model where the side and bottom surfaces of which are extended by 64km to the normal direction (See the summary of model settings in Table 1). On land, we used 1198 observation points, which were equivalent to the locations of GEONET observation points included in the target domain. On the seafloor, out of those serviced by the Japan Coast Guard and Tohoku University, the seven points that were studied in Sun et al. [17] were used.

As discussed previously, simulation results of postseismic crustal deformation are usually used in pointwise comparison with crustal deformation data. Note that a pointwise metric is stricter than the one based on integrated value, such as norm of displacement vector for whole the target domain, but proper for typical application problems such as inversion analysis of earthquake fault slip proposed by Yabuki & Matsu'ura [19]. Therefore, we evaluated the results at the locations of observation points where data for post seismic crustal deformation have been collected. This manner requires less postprocessing, and enables relatively clear visualization. For evaluation of convergence with respect to pointwise displacement, we seek to show that changes of computed displacements lie within a certain range when making changes to mesh size, time-step length and target domain. The term "certain range" refers to a relative difference of less than 1%. Here we define:

$$\varepsilon_a = |u'(\mathbf{r}) - u(\mathbf{r})|$$
$$\varepsilon_r = |\frac{u'(\mathbf{r}) - u(\mathbf{r})}{u(\mathbf{r})}|,$$

where ε_a, ε_r are absolute and relative differences, and $u(\mathbf{r})$ and $u'(\mathbf{r})$ are displacements in Point $\mathbf{r}$ computed with the basic settings and with the amended parameters. However, if the magnitude of the displacement is significantly small, the relative difference tends to be larger. It is therefore not always easy to evaluate these points using only relative difference. Hamanaka [7] reported that the observation errors of GEONET routine solutions are 2 mm horizontally and 1 cm vertically, which we used for evaluation of ε_a hereafter. Here, we determined that if the absolute value of the displacement is smaller than the observation error, the solution at that point is also included within the acceptable "certain range" without any additional conditions. In other words, at each observation point, the conditions

Horizontal:

Table 1: Comparison of the settings of the four models.

	ds	dt	area
Basic setting	1000m	30days	Figure1
Model A	750m	30days	Figure1
Model B	1000m	15days	Figure1
Model C	1000m	30days	Figure1+64km in the side and bottom planes

$$C_h^1 = (u < 200mm \ \wedge \ \varepsilon_a < 2mm)\,,$$
$$C_h^2 = (u \geq 200mm \ \wedge \ \varepsilon_r < 0.01)\,,$$
$$C_h^1 \ \vee \ C_h^2 = \{true\},$$

Vertical:

$$C_v^1 = (u < 1000mm \ \wedge \ \varepsilon_a < 10mm)\,,$$
$$C_v^2 = (u \geq 1000mm \ \wedge \ \varepsilon_r < 0.01)\,,$$
$$C_v^1 \ \vee \ C_v^2 = \{true\},$$

should be satisfied. Note that observation error is used only to decide which error to use as a metric for the evaluation, relative or absolute, and so we do not use any physical measurement values in this process. It is natural to introduce criteria which are coordinate-dependent, because errors in simulations or observations are sometimes coordinate-dependent (in our case, GEONET routine solutions error as mentioned above). The expressions are written in such a way that they are convenient for evaluation or visualization of differences, because all points are easily divided into two groups depending on the displacement value, as shown in the next section.

4 Results

Firstly we show the simulation results using HFM with the basic settings. The accumulated postseismic crustal deformation(coseismic + postseismic) for 10 years after the earthquake (including coseismic deformation) are shown in Figure 4. After the elastic response due to coseismic fault slip, viscoelastic response due to relaxation of stress merely contributes the difference of displacement between coseismic deformation and postseismic crustal deformation.

Next, we show the difference in the simulation results of the accumulated postseismic crustal deformation using models A, B and C. We plotted relative difference and absolute difference in the same figure because absolute error is used for checking the condition C_h^1 (or C_v^1) and relative error for C_h^2 (or C_v^2). Hence the observation points for checking C_h^1 and C_h^2 (or C_v^1 and C_v^2) do not overlap with each other. Relative error is plotted in blue and gold coloration, while absolute error is plotted in green and red. Since these two legends do not have common color with each other, the readers can judge which kind of error is being evaluated in a specific evaluation point only by its color. In cases where the value of the error was larger than the maximum value of the color bar in the legend, the point has been plotted in orange. Figure 5 illustrates the differences between the basic model and Model A. At almost all of the points, the difference is significantly small. In the z component, larger differences can be seen in seafloor observation points and in the Tohoku area. Figure 6 illustrates the differences between the basic

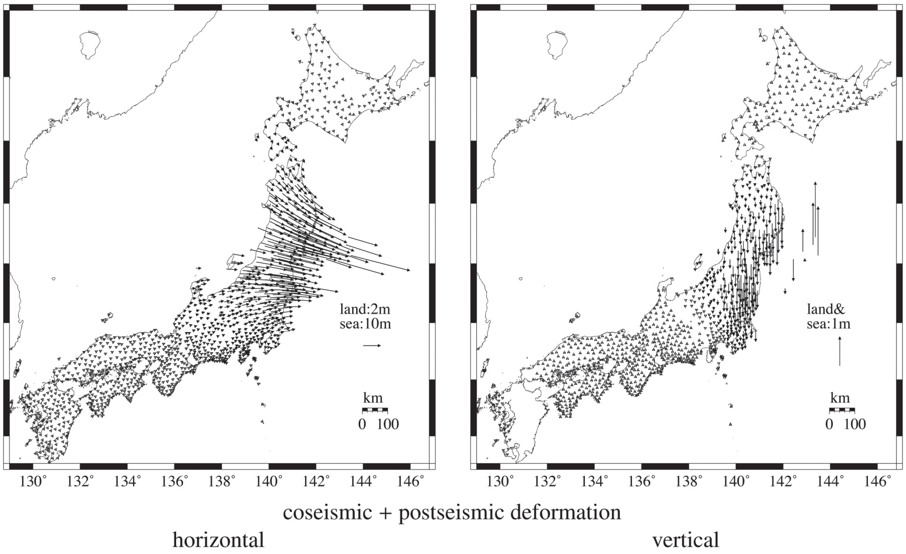
land:2m
sea:10m
land&
sea:1m
km
0 100
130° 132° 134° 136° 138° 140° 142° 144° 146°
coseismic + postseismic deformation
horizontal
vertical

Figure 4: Coseismic and postseismic deformation (10 years after the earthquake) due to earthquake fault slip computed by HFM. Note that the displacements are plotted in different scales according to their location, whether on the land and on the seafloor.

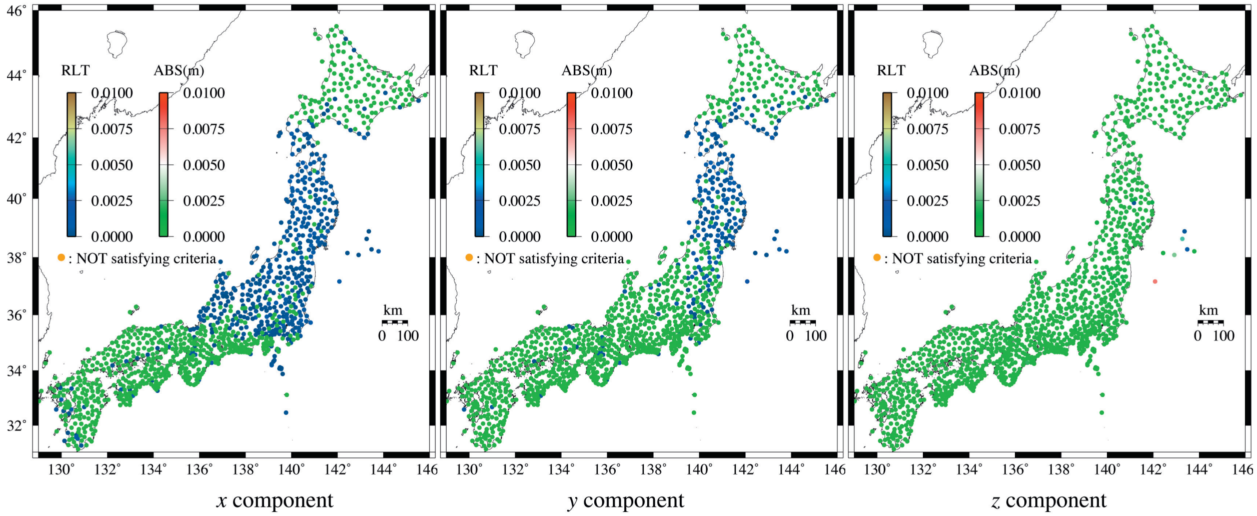
RLT
ABS(m)
0.0100
0.0075
0.0050
0.0025
0.0000
●: NOT satisfying criteria
km
0 100
46° 44° 42° 40° 38° 36° 34° 32°
130° 132° 134° 136° 138° 140° 142° 144° 146
x component
y component
z component

Figure 5: Comparison between the basic model and model A ($ds = 750$m). Relative error is plotted with a color legend of blue and gold, while absolute error green and red. In z component, larger differences can be seen in seafloor observation points and Tohoku area. There are no orange points, which means the numerical solution satisfies the criteria.

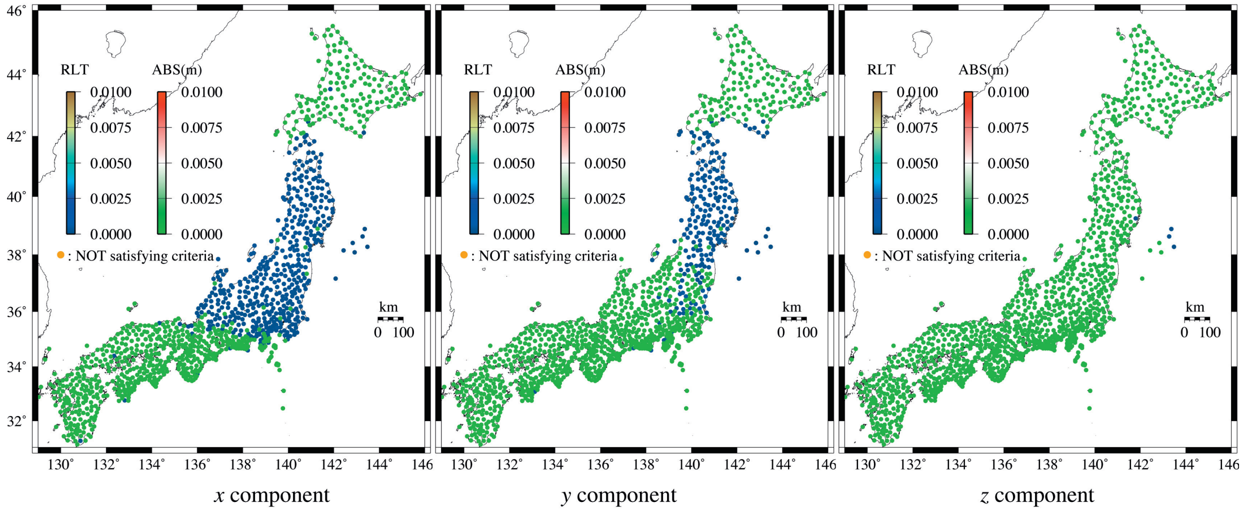
RLT
ABS(m)
0.0100
0.0075
0.0050
0.0025
0.0000
● : NOT satisfying criteria
km
0 100
46°
44°
42°
40°
38°
36°
34°
32°
130°
132°
134°
136°
138°
140°
142°
144°
146
x component
y component
z component

Figure 6: Comparison between the basic model and model B ($dt = 15$days). Relative error is plotted with a color legend of blue and gold, while absolute error green and red. Differece is significantly small in almost every point. There are no orange points, which means the numerical solution satisfies the criteria.

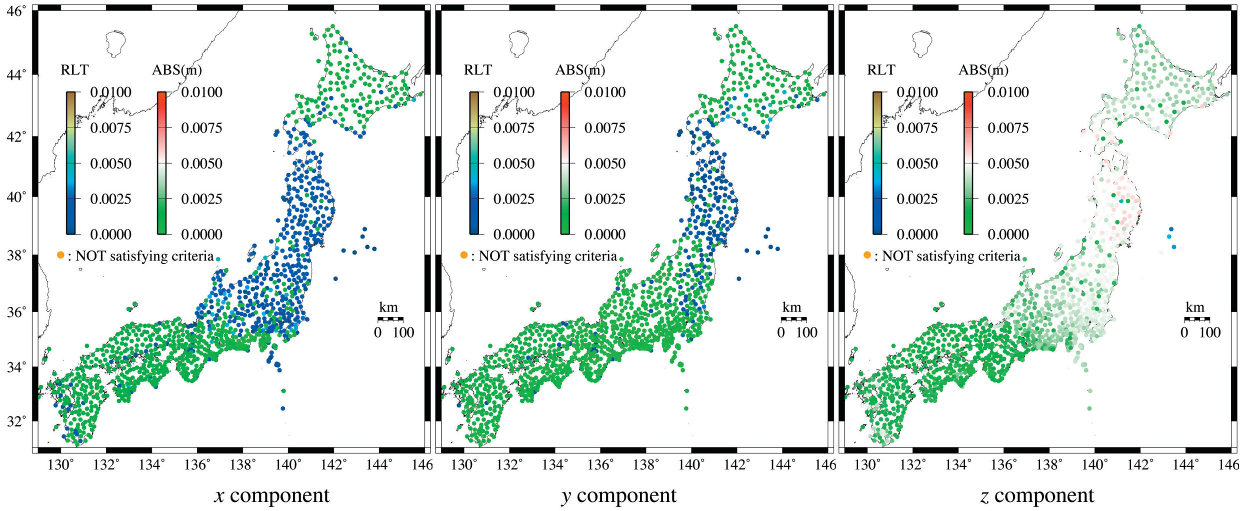
RLT
ABS(m)
0.0100
0.0075
0.0050
0.0025
0.0000
● : NOT satisfying criteria
km
0 100
46°
44°
42°
40°
38°
36°
34°
32°
130°
132°
134°
136°
138°
140°
142°
144°
146
x component
y component
z component

Figure 7: Comparison between the basic model and model C (boundaries are extended by 64km). Relative error is plotted with a color legend of blue and gold, while absolute error green and red. In the x component, larger difference can be seen in the locations far from the focal region than in the other components. There are no orange points, which means the numerical solution satisfies the criteria.

model and Model B. Again differences are significantly small at almost every point. Also, the influence of time-step length on these differences appears to be independent of point location. Figure 7 illustrates the differences between the basic model and Model C. In the x component, larger differences can be seen at locations far from the focal region than in the other components. This is probably because deformation in the x component is significantly larger than that of the other components (See Figure 4): The error due to the Dirichlet conditions imposed in the model boundaries may be expected to increase. Although the difference between these figures reflects the characteristics of the variable parameter, there are no orange points in any of the figures. This suggests that numerical solution of the basic model satisfies the criteria given in Section 3.

To compute a 10-year simulation using the basic model, we used 8192 nodes on K computer (1/10 of the entire resource) for 2.4 hours. It is clear that greater computation resources are needed for equivalent analyses using Models A, B and C due to their finer discretization or larger area. In addition, many prescribed analyses have been carried out for determining the basic system. These facts indicate that HPC techniques, which enable our scalable program to run on a state-of-the-art supercomputing system such as the K computer, are indispensable for this type of verification analysis.

5 Concluding remarks

Although verification, one of the two components of V&V,is important for assuring the quality of results obtained by numerical simulation, explicit verification has not been commonly applied to numerical simulation of crustal deformation. In this paper, we carried out numerical verification of the problem solved using HFM [9], by checking the convergence of numerical solutions with respect to mesh size, time-step length, and target domain. Since our computation method, specialized for an analysis in a large target domain, cannot apply widely used verification methods such as error analysis using Richardson extrapolation, we took another verification strategy. Specifically, considering the characteristics of crustal deformation simulation, we proposed verification criteria which used pointwise displacement for verification. In our criteria, the accuracy of the numerical solutions was explicitly shown by considering the observation error of the data used in validation. The computational time required for each analysis implies that HPC facilities are necessary for such verification, for crustal deformation analysis of the Japanese Islands. HPC in combination with such a verification method may be expected to assure the quality of crustal deformation simulations.

The quantity of crustal deformation data, in particular, seafloor observation data at high accuracy, is expected to increase in the future. Carrying out verification in simulations of crustal deformation will become more important in analysis of these data.

References

[1] B. T. Aagaard, M. G. Knepley, and C. A. Williams. A domain decomposition approach to implementing fault slip in finite-element models of quasi-static and dynamic crustal deformation. *Journal of Geophysical Research: Solid Earth*, 118(6):3059–3079, 2013.

[2] John G Anderson. Quantitative measure of the goodness-of-fit of synthetic seismograms. In *13th World Conference on Earthquake Engineering Conference Proceedings, Vancouver, Canada, Paper*, volume 243, 2004.

[3] Florent De Martin. Verification of a spectral-element method code for the southern california earthquake center loh. 3 viscoelastic case. *Bulletin of the Seismological Society of America*, 101(6):2855–2865, 2011.

[4] Yukitoshi Fukahata and Mitsuhiro Matsu'ura. Quasi-static internal deformation due to a dislocation source in a multilayered elastic/viscoelastic half-space and an equivalence theorem. *Geophysical Journal International*, 166(1):418–434, jul 2006.

[5] Geospatial Information Authority of Japan. Gnss earth observation network system. 2010.

[6] Chihiro Hashimoto, Kenji Fukui, and Mitsuhiro Matsufura. 3-D Modelling of Plate Interfaces and Numerical Simulation of Long-term Crustal Deformation in and around Japan. *Pure and Applied Geophysics*, 161(9-10):2053–2068, aug 2004.

[7] Y Hatanaka. Evaluation of Precision of Routine Solutions of GEONET (in Japanese). *Journal of the Geospatial Information Authority of Japan*, 108:49–56, 2005.

[8] T.J.R. Hughes, J.A. Cottrell, and Y. Bazilevs. Isogeometric analysis: Cad, finite elements, nurbs, exact geometry and mesh refinement. *Computer Methods in Applied Mechanics and Engineering*, 194(39–41):4135–4195, 2005.

[9] T. Ichimura, R. Agata, T. Hori, K. Hirahara, and M. Hori. On Analysis Method for Coseismic and Postseismic Crustal Deformation with Large-scale High-fidelity Model (preparing). *Geophysical Journal International*, 195(3), sep 2015.

[10] Y. Kaneda, K. Kawaguchi, E. Araki, H. Matsumoto, T. Nakamura, M. Nakano, S. Kamiya, K. Ariyoshi, T. Baba, M. Ohori, N. Takahashi, and T. Hori. Dense ocean floor network for earthquakes and tsunamis (donet/donet2) part3 –development and data application for the mega thrust earthquakes around the nankai trough–. 1:1553, 2011.

[11] K Koketsu, H Miyake, H Fujiwara, and T Hashimoto. Progress towards a Japan Integrated Velocity Structure Model and Long-Period Ground Motion Hazard Map. *The 14th World Conference on Earthquake Engineering*, pages 1–7, 2008.

[12] C. Kyriakopoulos, T. Masterlark, S. Stramondo, M. Chini, and C. Bignami. Coseismic slip distribution for the M w 9 2011 Tohoku-Oki earthquake derived from 3-D FE modeling. *Journal of Geophysical Research: Solid Earth*, 118(February):3837–3847, jul 2013.

[13] HJ Melosh and A Raefsky. A simple and efficient method for introducing faults into finite element computations. *Bulletin of the Seismological Society of America*, 71(5):1391–1400, 1981.

[14] Y Okada. Surface deformation due to shear and tensile faults in a half-space. *Bulletin of the Seismological Society of America*, 75(4):1135–1154, 1985.

[15] Jay Parker, Gregory Lyzenga, Charles Norton, Cinzia Zuffada, Margaret Glasscoe, John Lou, and Andrea Donnellan. Geophysical Finite-Element Simulation Tool (GeoFEST): Algorithms and Validation for Quasistatic Regional Faulted Crust Problems. *Pure and Applied Geophysics*, 165(3-4):497–521, may 2008.

[16] P. J. Roache. Quantification of Uncertainty in Computational Fluid Dynamics. *Annual Review of Fluid Mechanics*, 29(1):123–160, January 1997.

[17] Tianhaozhe Sun, Kelin Wang, Takeshi Iinuma, Ryota Hino, Jiangheng He, Hiromi Fujimoto, Motoyuki Kido, Yukihito Osada, Satoshi Miura, Yusaku Ohta, and Yan Hu. Prevalence of viscoelastic relaxation after the 2011 Tohoku-oki earthquake. *Nature*, 514:84–87, sep 2014.

[18] The American Society of Mechanical Engineers. Asme v&v 10-2006 - guide for verification and validation in computational solid mechanics. *The American Society of Mechanical Engineers*, 2006.

[19] T Yabuki and M Matsu'ura. Geodetic data inversion using a Bayesian information criterion for spatial distribution of fault slip. *Geophysical Journal International*, 109(2):363–375, 1992.

[20] Yuji Yagi and Yukitoshi Fukahata. Rupture process of the 2011 Tohoku-oki earthquake and absolute elastic strain release. *Geophysical Research Letters*, 38(19):1–5, 2011.

Acknowledgment

This work was supported by JSPS Fellows (26–8867). Part of the results is obtained by using the K computer at the RIKEN Advanced Institute for Computational Science (Proposal number hp120278 & 120308).